^{30}S studied with the ^{32}S(p, t)^{30}S reaction and the ^{29}P(p, γ)^{30}S reaction rate

D. W. Bardayan,[1] J. C. Blackmon,[1] R. P. Fitzgerald,[2] W. R. Hix,[1,3] K. L. Jones,[4,*] R. L. Kozub,[5] J. F. Liang,[1]
R. J. Livesay,[6] Z. Ma,[3] L. F. Roberts,[1] M. S. Smith,[1] J. S. Thomas,[4] and D. W. Visser[2]

[1]*Physics Division, Oak Ridge National Laboratory, Oak Ridge, Tennessee 37831, USA*
[2]*Department of Physics and Astronomy, University of North Carolina, Chapel Hill, North Carolina 27599, USA*
[3]*Department of Physics and Astronomy, University of Tennessee, Knoxville, Tennessee 37996, USA*
[4]*Department of Physics and Astronomy, Rutgers University, Piscataway, New Jersey 08854-8019, USA*
[5]*Physics Department, Tennessee Technological University, Cookeville, Tennessee 38505, USA*
[6]*Department of Physics, Colorado School of Mines, Golden, Colorado 80401, USA*

The ^{29}P(p, γ)^{30}S reaction rate affects the interpretation of nova Si abundances, which have been precisely measured in presolar grains. The rate is thought to be dominated by previously unobserved 3^+ and 2^+ resonances above the ^{30}S proton threshold at 4399 keV. To better understand the ^{29}P(p, γ)^{30}S rate, we have studied the ^{30}S nucleus with the ^{32}S(p, t)^{30}S reaction. We have observed 13 ^{30}S levels, nine of which are above the proton threshold, including a level at 4704 keV that is a candidate to be the important 3^+ resonance. We also resolve a significant discrepancy between previously published excitation energies. From the observed triton angular distributions, we constrain the spins of several levels, ruling out several previous hypotheses and constraining some for the first time. Using our updated information, we estimate the ^{29}P(p, γ)^{30}S reaction rate is approximately six times larger at nova temperatures than previously thought.

I. INTRODUCTION

Classical novae are powered by thermonuclear runaways that occur on the white dwarf component of close binary systems. During such violent stellar events, whose energy release is only exceeded by γ-ray bursts and supernova explosions, about 10^{-5} to 10^{-4} $M_\odot$ are ejected into the interstellar medium. Because of the mixing of the white dwarf matter and the high peak temperatures attained during the outburst, $T_{\text{peak}} \sim (1-4) \times 10^8$ K, the ejecta are enriched in nuclear processed material with abundances very different than those in the solar system. These nucleosynthetic signatures provide crucial benchmarks for nova models, which so far have not been able to completely explain observations [1].

One particularly promising technique for obtaining precise nova elemental (and even isotopic) abundances is the study of presolar grains in the laboratory. Ion microprobe analyses of single presolar grains have revealed a variety of isotopic signatures allowing the identification of parent stellar sources [2], and recently grains have been identified that are thought to be of nova origin [3]. These grains are characterized by low ^{12}C/^{13}C and ^{14}N/^{15}N ratios, ^{30}Si excesses, and close to or slightly lower than solar ^{29}Si/^{28}Si ratios. In some cases, high ^{26}Al/^{27}Al and low ^{20}Ne/^{22}Ne ratios have also been measured [3]. The silicon measurements are particularly important as the ^{29}Si and ^{30}Si abundances are good indicators of the peak temperatures achieved in the explosion and of the dominant nuclear paths followed in the course of the thermonuclear runaway, which have a clear imprint on the overall composition of the ejecta [4].

To interpret these precise Si abundance measurements, we must understand the rates of the thermonuclear reactions affecting Si production in novae. Particularly relevant are the ^{29}P(p, γ)^{30}S and ^{30}P(p, γ)^{31}S reactions. While there have been several recent studies of the ^{30}P(p, γ)^{31}S reaction rate [5–7], much less is known about the ^{29}P(p, γ)^{30}S reaction, which depending on its rate compared to the competing ^{29}P β^+ decay, directs the reaction flow toward ^{30}Si [via the ^{29}P(p, γ)^{30}S(β^+)^{30}P(β^+)^{30}Si sequence] and away from ^{29}Si, the product of ^{29}P β^+ decay. In fact, a recent sensitivity study found about a factor of 3 variation in the ^{29,30}Si abundances resulted when the ^{29}P(p, γ)^{30}S reaction rate was varied within prescribed limits [8]. The ^{29}P(p, γ)^{30}S reaction rate was also found to have significant effects on other nuclei produced in novae such as ^{31}P, ^{33}S, ^{34}S, ^{35}Cl, ^{36}Ar, ^{37}Ar, ^{37}Cl, ^{38}Ar, ^{39}K, and ^{40}Ca. Having a reliable calculation for the ^{29}P(p, γ)^{30}S reaction rate in novae is clearly important to understanding the nucleosynthesis occurring.

The astrophysical rate of the ^{29}P(p, γ)^{30}S reaction is, however, quite uncertain. The rate depends on properties of ^{30}S resonances above the proton threshold at $E_x = 4399 \pm 3$ keV. Evaluations [9,10] examining the known ^{30}S levels and those in the mirror nucleus ^{30}Si have concluded that the ^{29}P(p, γ)^{30}S reaction rate is dominated at nova temperatures by low-energy 3^+ and 2^+ resonances. Despite years of experimental study [11–18], however, evidence for the existence of these levels has never been published. Iliadis *et al.* [10] performed calculations using the isobaric multiplet mass equation estimating the 3^+ and 2^+ levels to be at 4733 and 4888 keV, respectively. Their calculations reproduced the energies for nine other isospin triplet states in ^{30}S on average within 40 keV, but others have estimated the actual uncertainties in the calculations to be closer to 100 keV [18]. Such uncertainties result in the

---

*Present address: Department of Physics and Astronomy, University of Tennessee, Knoxville, Tennessee 37996, USA.

^{29}P$(p, \gamma)^{30}$S reaction rate remaining uncertain by "orders of magnitude" [10].

II. REACTION STUDY

To better understand the level structure of ^{30}S and to search for these important levels, we have studied the ^{32}S$(p, t)^{30}$S reaction at the ORNL Holifield Radioactive Ion Beam Facility (HRIBF). Indirect studies such as this are critical for complementing direct measurements, and it is only through a combination of measurements and techniques that a truly complete reaction rate estimate can be made. Proton beams of 37 and 39 MeV were used to bombard ZnS targets, and tritons from the (p, t) reaction were detected and identified in the silicon detector array (SIDAR) [19]. The SIDAR is an annular array of silicon-strip detectors and was configured in "telescope" mode with 300-μm detectors backed by 500-μm detectors. Tritons were distinguished from other reaction products by standard energy-loss techniques similar to our previous study of the ^{28}Si$(p, t)^{26}$Si reaction [20,21]. The targets were produced by vacuum evaporation of ZnS powder onto carbon-coated glass slides. After deposition of the ZnS material onto the slides, carbon foils as thin as 1 μg/cm^2 (coated with ZnS) could be floated and picked up onto target frames. Unfortunately, some decomposition of the ZnS can occur during deposition, and thus the resulting foil may be nonstoichiometric [22]. This is not a concern here, however, because absolute cross sections were not needed to determine the energies of the observed ^{30}S levels and the shapes of the triton angular distributions produced by a particular angular-momentum transfer. Foils containing Zn on 11-μg/cm^2 parylene (C$_8$H$_8$) backings were

procured from Lebow Company [23] and used for background characterization.

III. DATA

Two sets of data were taken: the first used a 37-MeV proton beam to bombard a ~264-μg/cm^2 ZnS target on a 1-μg/cm^2 C backing with SIDAR covering $\theta_{lab} = 18°$–$48°$, the second used a 39-MeV proton beam to bombard a ~280-μg/cm^2 ZnS target on a 5-μg/cm^2 C backing with SIDAR covering $\theta_{lab} = 31°$–$75°$. Runs were also conducted with 250-μg/cm^2 Zn foils on 11-μg/cm^2 parylene (C$_8$H$_8$) backings for background calibrations. The beam current was continuously integrated from a thick graphite beam stop placed downstream of the target location. Typical triton energy spectra are shown in Fig. 1. At each angle, the top spectrum shown is that obtained with the ZnS target, while the shaded spectrum was from the Zn target. The main contaminants were observed with both targets and resulted from the ^{12}C$(p, t)^{10}$C(g.s.) and ^{16}O$(p, t)^{14}$O(g.s.) reactions. No other triton peaks were observed with the Zn target, indicating that reactions on the Zn component of the target only contributed a relatively flat background to our ^{32}S$(p, t)^{30}$S data. A few small peaks arising from the ^{34}S$(p, t)^{32}$S reaction were observed at the lowest angles and have been labeled as ^{32}S in Fig. 1. All other observed peaks are believed to be from the ^{32}S$(p, t)^{30}$S reaction. The energy resolution obtained was about 80 keV in the 37-MeV data and 120 keV in the 39-MeV data, mostly resulting from kinematic broadening due to the angular widths of the detector strips. Because of the poorer energy resolution and the factor of 5 increase in carbon contamination in the 39-MeV runs, these
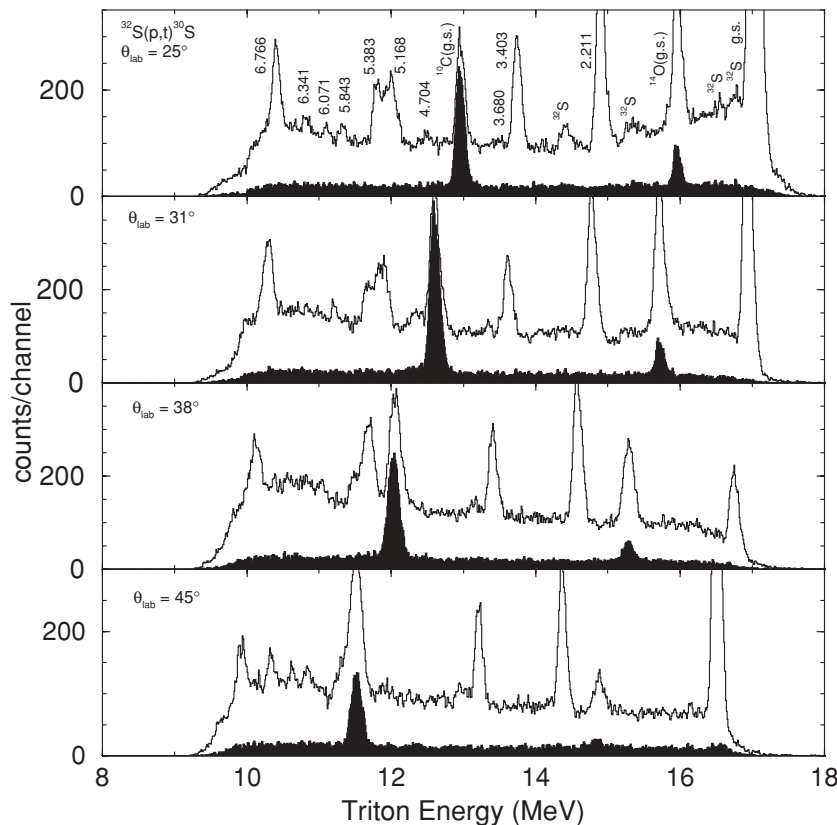
FIG. 1. Triton energy spectra shown at several angles. At each angle, the top spectrum is from reactions on the ZnS target while the shaded spectrum was obtained with the Zn target. Peaks are labeled with excitation energies in MeV from this work.

data were only useful for extending the angular distributions of strongly populated levels. All other spectroscopic information was taken from the 37-MeV data.

The ^{30}S peaks in Fig. 1 are labeled with excitation energies derived from our triton energy measurements. An internal energy calibration was performed using the well-known energies of low-lying states from previous γ-ray measurements [14]. This resulted in excitation energies for higher-lying states that agreed well with the previous data from Fynbo *et al.* but with a higher degree of uncertainty resulting from the extrapolation of the calibration to higher energies. We also considered using as a calibration point the 5842(4)-keV level previously observed by Fynbo *et al.* [17] and observed at all angles in our study. Excitation energies using both calibration methods agreed well, and so the average values were adopted and are shown in Table I along with those from the previous studies. Good agreement was obtained with the γ-ray measurements [14] at low excitation energies and those obtained from the

proton-decay measurements of Fynbo *et al.* [17] at higher energies. The excitation energies reported by Paddock [12] and Yokota *et al.* [15] seem to be systematically higher than the present results and those obtained by Fynbo *et al.* There is, of course, some ambiguity in the correspondence of states between the various studies, but we have assumed that the levels observed in Paddock's and our study are the same, because the same reaction was used at similar energies. The use of an internal calibration minimizes any effects of uncertainties in beam energy, target thickness, detector angles, and detector energy calibrations on the extracted excitation energies.

Of particular interest for the ^{29}P(p, γ)^{30}S reaction rate is the observation of a peak at 4704 ± 5 keV. While it was not particularly strong in this reaction, the peak was consistently visible in 10 of the 11 angles at which it was not blocked by the ^{12}C(p, t)^{10}C contamination line. There was also some indication of this peak in the data of Paddock (near channel 1600 in Fig. 4 of Ref. [12]), but the statistics there were

TABLE I. ^{30}S excitation energies in keV obtained in this work and previous works. If spin constraints were made, those are separated from the excitation energy by a dash. Uncertainties are shown in parentheses. In the present work, entries marked with a star (*) were used as calibration points in both sets of calibrations (see text).

Paddock [12] ^{32}S(p, t)^{30}S	Caraça *et al.* [13] ^{28}Si(^{3}He,$n\gamma$)^{30}S	Kuhlmann *et al.* [14] ^{28}Si(^{3}He,$n\gamma$)^{30}S	Yokota *et al.* [15] ^{28}Si(^{3}He,n)^{30}S(p)	Fynbo *et al.* [17] ^{31}Ar(β^+)^{31}Cl(p)^{30}S(p)	Present work ^{32}S(p, t)^{30}S
g.s. $- 0^+$					$0000(4) - 0^+$
2239(18) $- 2^+$	2209.9(11)	2210.7(5) $- 2$			2210.7* $- 2^+$
3438(14) $- 2^+$	3402.2(14)	3402.6(5) $- 1, 2$			3402.6* $- 2^+$
	3664.2(13)	3667.5(10)			
3707(25) $- (0^+)$		3676(3) $- 1$			3680(6) $- (1^+)$
					4704(5)
		5136(2) $- (4)$	5145(10)		
5207(22)					5168(6) $-$
					$4^+ + 0^+$
				5217.4(7)	
5306(25)			5288(10) $- 3^-$		
5426(25)			5425(10) $- (1,2)$	5389(2)	5383(8) $-$
					$(3^-,2^+)$
5897(27)			5912(10) $- (3,4)$	5842(4)	5843(5) $- (1^-)$
				(5945(3))	
(6108(29))			6117(10) $- 1^-,(2^+)$	6064(3)	6071(11)
(6223(30))			6233(10)	6202(3)	
				6280.1(12)	
6415(40)			6393(10) $- 0^+$	6338.6(14)	6341(5)
			6584(10) $- (2,3)$	6541(4)	6532(13)
				(6643(3))	
6861(40)			6810(10)	6762(4)	6766(10) $- 2^+$
			6838(10) $- \geqslant 4$	6855(4)	
			6919(10) $- (3,4)$	6927(4)	
7185(35)				7078(7)	7074(9)
			7133(10) $- (1,2)$	7123(10)	
				(7237(5))	
			7294(10) $- \geqslant 3$	7295(14)	
			7338(10) $- (1,2)$	7352(8)	
			7475(10)	7485(4)	
				7598(4)	
				7693(4)	
				7924(5)	

FIG. 2. Excitation energy extracted for the 4704-keV level as a function of detection angle assuming the observed peak was from the ^{32}S$(p, t)^{30}$S reaction. The kinematic lines demonstrate how the extracted excitation energy would change if the peak were really from reactions on other S isotopes populating states in ^{31,32}S, respectively.

FIG. 3. Triton angular distributions populating levels in ^{30}S, compared with DWBA curves for natural-parity levels and multistep FRESCO calculations for unnatural-parity levels.

$\sim$10 times less than in our study. It seems likely that the peak is due to a previously unobserved ^{30}S level and not a contaminant line for several reasons. First, no peaks appear at this energy in the Zn target runs, and thus the origin of the peak in the ZnS runs cannot be from reactions on the Zn, C, or O in the target. Next, the centroid of the peak shifts in energy as one would expect kinematically for the ^{32}S$(p, t)^{30}$S reaction. We plot in Fig. 2, the extracted excitation energy of the peak assuming it was produced by the ^{32}S$(p, t)^{30}$S reaction as a function of detection angle. If the correct reaction was assumed to produce the peak, then the extracted excitation energies should not change with angle. If, on the other hand, the peaks were actually from reactions on other S isotopes, then the extracted excitation energy would appear to shift lower as a function of angle. As can be seen in Fig. 2, the data are fit best by the ^{32}S$(p, t)^{30}$S kinematics line. Finally, ^{33,34}S are minor contaminants in the target having only 0.75% and 4.21% natural abundances, respectively. While there is evidence for ^{34}S$(p, t)^{32}$S peaks at the lowest angles, reactions on ^{33}S should be down farther in yield by another factor of $\sim$5 from those on ^{34}S. The only hypothesis consistent with these arguments is that the peak is from a previously unknown ^{30}S level at 4704 keV. This energy is consistent with the expected 3^+ level estimated to be at 4733 keV by Iliadis *et al.* [10] or somewhat less likely is the expected 2^+ level that was estimated to be at 4888 ± 100 keV (here we quote the more conservative uncertainties adopted by Ref. [18]). No other levels are expected within $\sim$300 keV.

IV. ANALYSIS OF ANGULAR DISTRIBUTIONS

Angular distributions were extracted for strongly populated ^{30}S levels and are plotted in Fig. 3. Gaps appear in the angular distributions where the peak of interest was obscured by a contaminant peak, or if tritons populating the state did not
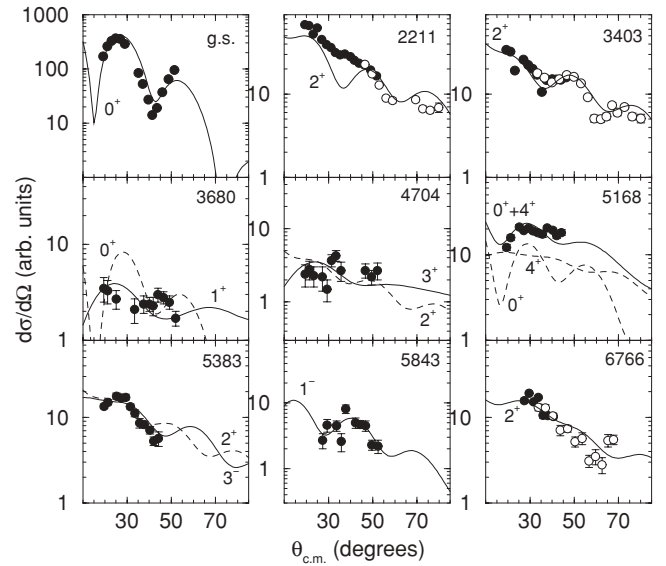
stop in the E detector. The filled and open circles are data from the 37- and 39-MeV runs, respectively. Good agreement was observed at the common angles of the two sets of runs. The vertical scale of Fig. 3 is in μb/sr but is labeled as arbitrary units since the exact target stoichiometry could not be determined (see above discussion). As mentioned previously, knowing the absolute amount of ^{32}S in the target was not necessary, since only the relative triton energies and angular distributions were needed in this study.

The angular distributions were compared to calculations using the distorted-wave Born approximation (DWBA) finite-range code DWUCK5 [24] for natural-parity levels and the coupled-channels code FRESCO [25] for unnatural-parity levels. In a simple shell-model picture, the valence neutrons would occupy and fill the $2s_{1/2}$ shell. Thus for excited 0^+ states, transfers of pairs from the $2s_{1/2}$, $1d_{5/2}$, and $1p_{1/2}$ orbitals were considered, with the best results coming from transfers from $2s_{1/2}$ orbitals. For 2^+ and 4^+ final states, it was assumed in the calculations that the neutron pair was transferred from the $1d_{5/2}$ shell. The only exception to this was for the 2211-keV state, which is known to have a $2s_{1/2}$-$1d_{3/2}$ dominant configuration [16]. For odd-parity states, the calculations were done for one neutron transferred from the $1d_{5/2}$ or $2s_{1/2}$ shell plus one from either the $1p_{1/2}$ or $1p_{3/2}$ shell. Except for 0^+ final states, the shapes of the calculated angular distributions were relatively insensitive to the particular choice of shell-model orbitals. For unnatural-parity levels, multistep processes have to be considered. We have, therefore, performed FRESCO calculations of the expected angular distributions for the sequence ^{32}S$(p, d)^{31}$S$^{g.s.}(d, t)^{30}$S. Such multistep processes have been found to be important in other (p, t) studies populating unnatural-parity levels [26,27]. Optical model parameters were taken from Ref. [28] for protons and deuterons and Ref. [24] for tritons. The proton real well depth was modified slightly to better reproduce the

TABLE II. Optical model parameters used in the analysis of the angular distributions were taken from Refs. [24,28].

Particle	V_R (MeV)	V_I (MeV)	$4W_D$ (MeV)	r_R (fm)	a_R (fm)	r_I (fm)	a_I (fm)	$\lambda_{s.o.}$
p	37.1		27.5	1.18	0.66	1.18	0.66	
d	90.0		100.0	1.30	0.62	1.18	0.58	
t	144	30		1.24	0.678	1.45	0.841	
n				1.25	0.65			25

angular distributions for the lowest-lying levels. Other optical model parameter sets were also considered (e.g., Becchetti and Greenlees [29]), but better fits were not obtained. The final optical model parameters used as well as the bound state potential parameters are given in Table II.

V. RESULTS FOR INDIVIDUAL LEVELS

The ground state. Tritons populating the ^{30}S ground state were observed in the 37-MeV data but were too energetic to be stopped in the 39-MeV data. The ground state has $J^\pi = 0^+$, and the angular distribution is well described by an $\ell = 0$ transfer.

The 2211-keV level. The 2211-keV level is known to be a 2^+ from previous transfer reaction angular distributions (e.g., Refs. [11,12]) and n-γ angular correlation studies [14]. Our triton angular distribution is reasonably consistent with an $\ell = 2$ transfer, but similar to what was observed by Paddock [12], the DWBA calculation of a dip around $\theta_{\text{c.m.}} = 35°$ is not confirmed by the data.

The 3403-keV level. Similar to the 2211-keV level, this state is known to be a 2^+ from angular distributions measured in transfer reactions. Our measured triton angular distribution is fit well by an $\ell = 2$ transfer.

The 3680-keV level. We observe a level at 3680 ± 6 keV in our study that most likely corresponds to the 3676 ± 3 keV level observed by Kuhlmann *et al.* [14] and the 3707 ± 25 keV level observed by Paddock [12]. Paddock had tentatively assigned this level as 0^+, but the results were not conclusive because of the relatively poor statistics. Kuhlmann *et al.* found, however, that their n-γ correlations were fit much better by a $J = 1$ assignment. The only possible ^{30}Si mirror level has $J^\pi = 1^+$, and so they show the level as $1^{(+)}$ in their Fig. 8 [14]. Our measured triton angular distribution does not agree with a 0^+ assignment but is relatively consistent with the FRESCO calculation for a 1^+ angular distribution. We therefore support the 1^+ assignment.

The 4704-keV level. We observe a previously unknown level at 4704 ± 5 keV. This level is most likely the mirror to the 3^+ ^{30}Si level at 4831 keV, which has been estimated to be at 4733 keV in ^{30}S by Iliadis *et al.* [10]. It could also possibly be the 2^+ level estimated by Iliadis *et al.* to be at 4888 keV, but this seems less likely considering how well the calculations reproduce other ^{30}S energies. The uncertainties in these calculations are estimated to be 40–100 keV [8,18]. No other ^{30}S levels are expected within ± 300 keV. The angular distribution for this level is relatively consistent with either assignment.

The 5168-keV level. We observed a peak corresponding to a ^{30}S excitation energy of 5168 ± 6 keV. This is most likely part of an unresolved doublet. Kuhlmann *et al.* [14] and Yokota *et al.* [15] observed levels at 5136 ± 2 and 5145 ± 10 keV, respectively. Higher-energy levels have been observed by Paddock [12] at 5207 ± 22 keV and Fynbo *et al.* [17] at 5217.4 ± 0.7 keV. The only constraints on the spin come from the study of Kuhlmann *et al.* who conclude the 5136-keV level is most likely a 4^+. In the subsequent analysis by Wiescher and Görres [9], they conclude there are most likely at least two levels near this energy: a 4^+ at 5145 keV and a 0^+ near 5.2 MeV. Our triton angular distribution could not be fit with a single angular momentum transfer but was best fit with a combination of $\ell = 0$ and $\ell = 4$ angular momentum transfers indicating that this peak is probably an unresolved doublet.

The 5383-keV level. We extract an energy of 5383 ± 8 keV for this level. The state was previously observed by Paddock [12] at 5426 ± 25 keV, by Yokota *et al.* [15] at 5425 ± 10 keV, and by Fynbo *et al.* [17] at 5389 ± 2 keV. The only previous constraints on the spin come from the Yokota *et al.* study where it was tentatively assigned as $J = 1$ or 2. Our measured triton angular distribution is best fit by an $\ell = 3$ angular momentum transfer, but $\ell = 2$ would also be reasonably consistent. The most likely conclusion is that the 5383-keV level is the mirror to the 2^+ ^{30}Si level at 5614 keV. This is supported by the strong evidence from Yokota *et al.* that the mirror to the 3^- ^{30}Si level at 5488 keV is lower in energy at 5288 ± 10 keV in ^{30}S with no other 3^- levels expected in this excitation energy region.

The 5843-keV level. We observe a peak at 5843 ± 5 keV. Previously Paddock [12] found 5897 ± 27 keV and Fynbo *et al.* [17] found 5842 ± 4 keV. Yokota *et al.* [15] observed a level at 5912 ± 10 keV, but it is unclear if this is the same level. The triton angular distribution was best fit by an $\ell = 1$ transfer, but because of the relatively poor statistics obtained for this level, we cannot rule out $\ell = 2, 3, 4$.

The 6071-, 6341-, and 6532-keV levels. We observed levels at 6071 ± 11 keV, 6341 ± 5 keV, and 6532 ± 13 keV. These most likely correspond to levels observed by Fynbo *et al.* [17] at 6064 ± 3 keV, 6338.6 ± 1.4 keV, and 6541 ± 4 keV, respectively. These levels were all too weak to extract reasonable angular distributions.

The 6766-keV level. We extract an excitation energy of 6766 ± 10 keV for this level that was observed previously by Fynbo *et al.* [17] at 6762 ± 4 keV and Paddock [12] at 6861 ± 40 keV. No previous spin assignments have been made. Our triton angular distribution is best fit by an $\ell = 2$ angular momentum transfer.

The 7074-keV level. We observe a level at 7074 ± 9 keV that most likely corresponds to the level observed by
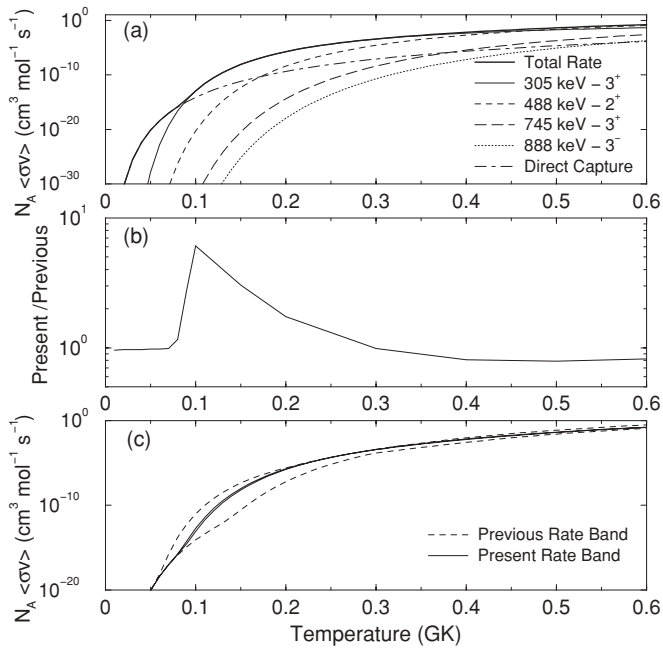
FIG. 4. (a) Updated ^{29}P$(p,\gamma)^{30}$S reaction rate. The 3^+ resonance dominates the rate over the nova temperature range. (b) Ratio of present to previous reaction rate. The present rate is up to six times larger than the rate in Ref. [10] at nova temperatures owing to the reduced energy of the important 3^+ resonance. (c) Variation in the calculated reaction rate due to the uncertainty in the 3^+ resonance energy as a function of temperature.

Fynbo *et al.* [17] at 7078 ± 7 keV and by Paddock [12] at 7185 ± 35 keV. Because of the energy required to punch through the ΔE detector, this level was only observed in our 39-MeV data and thus only at rather large angles. We, therefore, could not extract a reasonable angular distribution to provide a spin constraint.

VI. REACTION RATE

We update the calculated ^{29}P$(p,\gamma)^{30}$S reaction rate from Iliadis *et al.* [10] in Fig. 4. The only modification to the resonance parameters is to update the energy of the important 3^+ resonance to 305 ± 6 keV (from 333 ± 100 keV in Ref. [10]) and to scale the proton width to 2.8×10^{-5} eV (from 9.1×10^{-5} eV in Ref. [10]). The ^{29}P$(p,\gamma)^{30}$S reaction is dominated at peak nova temperatures (0.1–0.4 GK) by this 3^+ resonance. At temperatures below 0.1 GK, the rate is thought to be dominated by direct capture, which we take from Wiescher and Görres [9]. The present rate is approximately six times larger than the Iliadis *et al.* rate at 0.1 GK owing to the lower energy of the 3^+ resonance. Other resonances than those plotted in Fig. 4 provide negligible contributions in the nova temperature range.

In Fig. 4(c), we show the effect the previous ± 100 keV uncertainty had on the calculated ^{29}P$(p,\gamma)^{30}$S reaction rate (e.g., a factor of 4000 variation in the rate at 0.13 GK). In comparison, the present resonance energy uncertainty results in at most a factor of 2 variation in the rate.

We investigated the nova nucleosynthesis of Si isotopes with the updated ^{29}P$(p,\gamma)^{30}$S reaction rate by using the framework available through the Computational Infrastructure for Nuclear Astrophysics [30]. A "post-processing" approach, similar to that is Ref. [31], was utilized following a reaction rate network through time profiles of temperature and density in 28 radial zones taken from one-dimensional hydrodynamic calculations of nova outbursts [32]. A full reaction rate network was used in each zone with 169 isotopes from ^{1}H to ^{54}Cr. Reaction rates were taken from the NACRE evaluation in Ref. [33] where available and otherwise from the REACLIB database [34]. The only exceptions were for the ^{29}P$(p,\gamma)^{30}$S rate, which was taken from this work, and the ^{30}P$(p,\gamma)^{31}$S rate, which was taken from Ref. [5] and is similar to the one in Jenkins *et al.* [6]. Final abundances were determined by summing the contributions of each zone weighted by the total mass of the zone divided by the total mass of the ejected envelope. Thermodynamic profiles were taken from hydrodynamical simulations of ONeMg novae on white dwarf stars with masses of 1.15, 1.25, and 1.35 solar masses. We find that ^{30}Si is significantly enhanced in our calculations compared to solar values. The ^{30}Si/^{28}Si ratio was approximately 10, 12, and 17 times the solar value in the 1.15, 1.25, and 1.35 solar mass models, respectively. ^{29}Si/^{28}Si ratios were, however, near the solar value. Such a signature is consistent with abundance observations of presolar grains identified to have a nova origin, and our calculations support this explanation. Additionally, we find that the previous ± 100 keV uncertainty in the 3^+ resonance energy resulted in a factor of 1.4 variation in the calculated ^{29}Si/^{28}Si abundance ratio, while the present energy uncertainty has essentially no effect.

VII. CONCLUSIONS

In conclusion, we have studied astrophysically important ^{30}S levels with the ^{32}S$(p,t)^{30}$S reaction. We have observed 13 levels, nine of which are above the proton threshold including a previously unobserved level at 4704 keV. This level is most likely a "missing" 3^+ level expected near 4733 keV. Our measurements also clear up a significant discrepancy in the energies of higher lying levels, agreeing with the more recent measurement of Fynbo *et al.* [17] and disagreeing with the earlier values from Paddock [12] and Yokota *et al.* [15]. We additionally rule out the previous hypothesis of 0^+ for the 3680-keV level by Paddock [12], and we support the 1^+ assignment made by Kuhlmann *et al.* [14]. We provide experimental evidence for an unresolved $4^+/0^+$ doublet near 5168 keV that was previously hypothesized by Wiescher and Görres [9]. We rule out the 1^- possibility suggested by Yokota *et al.* [15] for the 5383-keV level indicating the level is most likely a 2^+. We additionally provide the first constraints on the spin of the 6766-keV level. Our results agree well with previous measurements for other levels. Using our results, we have updated the ^{29}P$(p,\gamma)^{30}$S reaction rate calculation and find it to be larger than the previous calculation [10] by as much as a factor of 6 at 0.1 GK. The uncertainty in the reaction rate resulting from the uncertain 3^+ resonance energy has been reduced from a factor of 4000 to a factor of 2. Nucleosynthesis

calculations generally support the view that certain presolar grains with large ^{30}Si excesses can be produced in massive novae.

[1] S. Starrfield, Phys. Rep. **311**, 371 (1999).
[2] E. Zinner, Annu. Rev. Earth Planet Sci. **26**, 147 (1998).
[3] S. Amari, X. Gao, L. R. Nittler, E. Zinner, J. José, M. Hernanz, and R. S. Lewis, Astrophys. J. **551**, 1065 (2001).
[4] J. José, M. Hernanz, S. Amari, K. Lodders, and E. Zinner, Astrophys. J. **612**, 414 (2004).
[5] Z. Ma *et al.*, Phys. Rev. C **76**, 015803 (2007).
[6] D. G. Jenkins *et al.*, Phys. Rev. C **73**, 065802 (2006).
[7] C. Wrede, J. A. Caggiano, J. A. Clark, C. Deibel, R. Lewis, A. Parikh, P. D. Parker, and C. Westerfeldt, Bull. Am. Phys. Soc. **52**, No. 3, 139 (2007).
[8] C. Iliadis, A. E. Champagne, J. José, S. Starrfield, and P. Tupper, Astrophys. J. Suppl. Ser. **142**, 105 (2002).
[9] M. Wiescher and J. Görres, Z. Phys. A **329**, 121 (1988).
[10] C. Iliadis, J. M. D'Auria, S. Starrfield, W. J. Thompson, and M. Wiescher, Astrophys. J. Suppl. Ser. **134**, 151 (2001).
[11] W. R. McMurray, P. Van Der Merwe, and I. J. Van Heerden, Nucl. Phys. **A92**, 401 (1967).
[12] R. A. Paddock, Phys. Rev. C **5**, 485 (1972).
[13] J. M. G. Caraça, R. D. Gill, A. J. Cox, and H. J. Rose, Nucl. Phys. **A193**, 1 (1972).
[14] E. Kuhlmann, W. Albrecht, and A. Hoffmann, Nucl. Phys. **A213**, 82 (1973).
[15] H. Yokota, K. Fujioka, K. Ichimaru, Y. Mihara, and R. Chiba, Nucl. Phys. **A383**, 298 (1982).
[16] L. Kraus *et al.*, Phys. Rev. C **37**, 2529 (1988).
[17] H. O. U. Fynbo *et al.*, Nucl. Phys. **A677**, 38 (2000).
[18] D. Galaviz *et al.*, in Proceedings of Science: International Symposium on Nuclear Astrophysics — Nuclei in the Cosmos — IX, PoS(NIC-IX) 099.
[19] D. W. Bardayan *et al.*, Phys. Rev. Lett. **83**, 45 (1999).
[20] D. W. Bardayan *et al.*, Nucl. Phys. **A718**, 505c (2003).
[21] D. W. Bardayan *et al.*, Phys. Rev. C **65**, 032801(R) (2002).
[22] J. Heagney (private communication).
[23] Lebow Company, Goleta, CA.
[24] P. D. Kunz, University of Colorado (http://spot.colorado.edu/~kunz/DWBA.html).
[25] I. J. Thompson, Comput. Phys. Rep. **7**, 167 (1988).
[26] D. W. Bardayan *et al.*, Phys. Rev. C **74**, 045804 (2006).
[27] N. B. de Takacsy, Nucl. Phys. **A231**, 243 (1974).
[28] R. L. Kozub, Phys. Rev. **172**, 1078 (1968).
[29] F. D. Becchetti, Jr. and G. W. Greenlees, Phys. Rev. **182**, 1190 (1969).
[30] http://nucastrodata.org
[31] S. Parete-Koon *et al.*, Astrophys. J. **598**, 1239 (2003).
[32] S. Starrfield *et al.*, Mon. Not. R. Astron. Soc. **296**, 502 (1998).
[33] C. Angulo *et al.*, Nucl. Phys. **A656**, 3 (1999).
[34] T. Rauscher and F.-K. Thielemann, At. Data Nucl. Data Tables **79**, 47 (2001).